



## Dielectric Behavior of M-Type Hexaferrites $\text{Sr}_{1-x}\text{Dy}_x\text{Fe}_{12}\text{O}_{19}$ Doped with Rare Earth Ions

Arun Katoch<sup>\*</sup>, B.K.Borthakur<sup>\*</sup>, Anterpreet Singh<sup>\*\*</sup> and Taminder Singh<sup>\*\*\*</sup>

<sup>\*</sup>Department of Physics, CMJ University, Meghalaya, India.

<sup>\*\*</sup>Department of Applied Sciences, BKSJ Engineering College, Amritsar, India.

<sup>\*\*\*</sup>Department of Physics, Khalsa College, Amritsar, India.

(Received 15 December, 2012, Accepted 2 January, 2013)

**ABSTRACT:** Dielectric properties have been studied for a series of M-type spinel hexagonal ferrite samples with the composition of  $\text{Sr}_{1-x}\text{Dy}_x\text{Fe}_{12}\text{O}_{19}$  ( $x = 0.0, 0.10, 0.20, 0.30$  and  $0.40$ ) have been prepared by employing the ceramic technique, as a function of frequency and temperature. The structural properties of the calcined samples were studied using X-ray diffraction (XRD), SEM technique. The samples were sintered at  $1150^\circ\text{C}$  for 8 hours. The X-ray diffraction patterns shows that the prepared samples have a single phase. The lattice parameters 'c' and 'a' was found to decreases by increasing Dy-content whereas the X-ray density increases by increasing Dy-content. Microstructural analysis by scanning electron microscopy (SEM) suggest that the compound have small grains distributed uniformly and non-uniformly on the surface of the sample and also shows that the grain size has been decreased by increasing the Dy-content in the composition  $\text{Sr}_{1-x}\text{Dy}_x\text{Fe}_{12}\text{O}_{19}$ . The dispersion of dielectric constant was discussed in the light of Koops model and hopping conduction mechanism. The dielectric loss tangent ( $\tan \delta$ ) curves exhibits a dielectric relaxation peaks which are attributed to the coincidence of the hopping frequency of the charge carriers with that of the external field. The dielectric constant and dielectric loss tangent were found to increase with increasing the temperature due to the increase of the hopping frequency, while they decrease with increasing Dy ion content due to the reduction of iron ions available for the conduction process. The variation of dielectric constant ( $\epsilon'$ ) and loss tangent ( $\tan \delta$ ) in the frequency range 1KHz to 1MHz were studied. The conduction phenomenon on was explained on the basis of a small polaron hopping model.

**Keywords:** Hexagonal ferrites, X-ray diffraction, SEM, Dielectric Constant ( $\epsilon'$ ) and Dielectric loss tangent ( $\tan \delta$ )

### I. INTRODUCTION

Ferrites continue to be very attractive materials for technological applications due to their electrical and dielectric properties. Most of the investigations carried out on ferrites with the M-type crystalline structure.  $\text{AF}_{12}\text{O}_{19}$  with  $A = \text{Ba}, \text{Sr}, \text{Dy}$  have been mainly devoted to Ba and Sr-based compounds. Hexagonal ferrites have several applications from microwave to radio frequency range. Several studies on the magnetic properties for hexagonal ferrites have also been reported [1-4]. Magnetic materials are found in home appliances, electronic products, communication equipment and data-processing devices. Ferrites are used also in radio and television, microwave and satellite communications. A few studies are available on non-magnetic properties such as dielectric properties for hexagonal ferrites [5-8]. Their electrical and dielectric properties depends on the preparation condition, such as sintering temperature, sintering atmosphere and the soaking time as well as the type of the substituted ions.

Hexagonal strontium ferrites have been intensively investigated during the last few decades due to their considerable importance to the electronic material industry. The hexagonal Barium (BaM) and Strontium ferrite (SrM) is considered to be an excellent candidate for magnetic recording media and characterized with high magnetocrystalline anisotropy, moderate hard magnetic properties and high chemical stability, compared with other magnetic materials. The common processing methods of hexagonal ferrites are conventional ceramic process of solid-state reaction [7], co-precipitation method [8], sol-gel process [9] and molten salt method [9,10] etc. The conventional ceramic process, which includes the mixing the raw materials, calculation, milling, pressing and sintering at  $1150\text{-}1200^\circ\text{C}$  [11]. In a fine particle form, Strontium ferrite is suitable for high-density recording media. Ultrafine strontium ferrite powder with narrow particle size distribution is desirable to increase the

capacity of information storage as well as to reduce the medium noise [12].

The aim of this work is to study the effect of Dy ion substitution on the behavior of dielectric properties of  $\text{Sr}_{1-x}\text{Dy}_x\text{Fe}_{12}\text{O}_{19}$  at different frequencies and temperatures. Structural properties and particle size of hexaferrite were also investigated by XRD, SEM.

## II. EXPERIMENTAL PROCEDURE

### A. Sample Preparation

All the samples of Sr-hexaferrites ( $\text{SrFe}_{12}\text{O}_{19}$ ) of nominal composition ( $x = 0.0, 0.10, 0.20$  and  $0.30$ ) were synthesized starting from ball-milling mixtures of  $\text{SrCO}_3$ ,  $\text{Fe}_2\text{O}_3$  and Dy-rare earth ion for 12h. After drying at  $60^\circ\text{C}$  for 6h, the powder mixture was heated at temperature of  $800\text{--}1150^\circ\text{C}$  for 4 h in a lid-covered alumina crucible with a heating rate of  $5^\circ\text{C}/\text{min}$  in air. Then after cooling to room temperature in furnace. In order to make the sintered magnet, the Strontium ferrite powder were wet mixed in acetone medium with addition of 4% polyvinyl alcohol (PVA) binder solution by using a ball mill. The mixture were reground again for 5h and the final fine powder were pressed in disk-shaped pellets with thickness ranging from 2mm to 4mm and with diameter from 7mm to 9mm. Then the pellets were sintered in a resistance heated furnace for 3h at each specified level of sintering temperature from  $950$  to  $1250^\circ\text{C}$ . The samples were slowly cooled to room temperature.

### B. Characterization

Structural characterization was carried out by X-ray diffraction (XRD), Scanning electron microscope (SEM). The crystal structure of the samples was examined by using a X-ray Diffractometer (XPRT-PRO) with  $\text{CuK}(\lambda = 1.5406)$  radiations which confirmed the formation of hexagonal structure with a few peaks of ( $-\text{Fe}_2\text{O}_3$ ). Theoretical X-ray density (T.D.) is calculated using formula

$$\text{T.D} = \frac{2nM}{\sqrt{3}.N_a a^2 c} \quad \dots(1)$$

where  $n$  is number of atoms,  $M$  is molecular weight,  $N_a$  is Avogadro's number per gram mole and 'a' and 'c' are lattice constants.

Experimental or bulk X-ray density (B.D.) is measured using Archimedes principle.

Let  $W_1$  = Weight of ferrite sample in water

$W_2$  = Weight of ferrite sample in air

Thus, Bulk density = (Weight in air) / (Weight in air-Weight in water)

Mathematically it can be written as

$$\text{B.D} = W_2 / (W_2 - W_1) \quad \dots(2)$$

From the X-ray density and bulk density of the sample, the percentage porosity of the sample has been calculated from following relation

$$P = (\text{T.D}-\text{B.D})/\text{T.D} \times 100\% \quad \dots (3)$$

The physical and mechanical properties are strongly influenced by their microstructure, so their studies are essential to understand the relationship between the processing parameters as well as the behavior of the materials when used in practical applications. In the present study, a JEOL-JSM 6100 scanning electron microscope was employed to examine the microstructural features such as grain size and porosity. The line intercept method [13] was used to measure the grain size. For the purpose of more accuracy, at least 10 grains were measured at different sections of each sample. Similar result and reason have been reported by Hussain *et. al.* [14]. The dielectric properties such as Dielectric constant ( $\epsilon'$ ) and loss tangent ( $\tan \delta$ ) of all the samples were measured by HP4284A precision LCR meter having frequency range from 20 Hz-1MHz. All the measurements have been carried by using a cell having platinum electrodes.

## III. RESULT AND DISCUSSION

### A. Phase Identification

Fig . 1 shows the XRD pattern obtained for different molar concentration in the prepared samples of  $\text{Sr}_{1-x}\text{Dy}_x\text{Fe}_{12}\text{O}_{19}$  ferrites sintered at  $1250^\circ\text{C}$  for 6h. This analysis reveals that the prepared samples were almost single hexagonal M-type Phase. In case of  $\text{Dy}^{3+}$  series, all peaks correspond to hexaferrites, however for the substitution  $x = 0.30$ , extra peaks of hematite ( $-\text{Fe}_2\text{O}_3$ ) and tetragonal  $\text{Sr}_3\text{Fe}_2\text{O}_7$  are observed. This indicates that Dy for  $x = 0.30$  did not substitute totally into the Sr M-type structure resulting in incomplete reactions between  $\text{Fe}^{3+}$  and  $\text{Sr}^{2+}$ , indicated by tracing of secondary phases in these samples, and is attributed to the preparation process. The respective peaks show that a magnetoplumbite structure has been formed. The variation in relative intensities of peaks may be related to the occupation of lattice sites by substituted ions. The lattice constants 'a' and 'c' with composition (x) for  $\text{Sr}_{1-x}\text{Dy}_x\text{Fe}_{12}\text{O}_{19}$  has been decreases continuously with increasing substituted amount of Dy ions. The peak for the doped strontium ferrites appears at the same position as for undoped ferrite, with different intensities. The result indicates that the formation of temperature of  $\text{Sr}_{1-x}\text{Dy}_x\text{Fe}_{12}\text{O}_{19}$  is about  $1250^\circ\text{C}$ . It is about  $50^\circ\text{C}$  higher than that of classical ceramic method for undoped strontium ferrite as indicated in the literatures. In the doped ferrites cases, the dopant of  $\text{Dy}^{2+}$  seem to dissolve / arrange in the

hexagonal structure to fulfill the formation of single hexagonal phase [15].

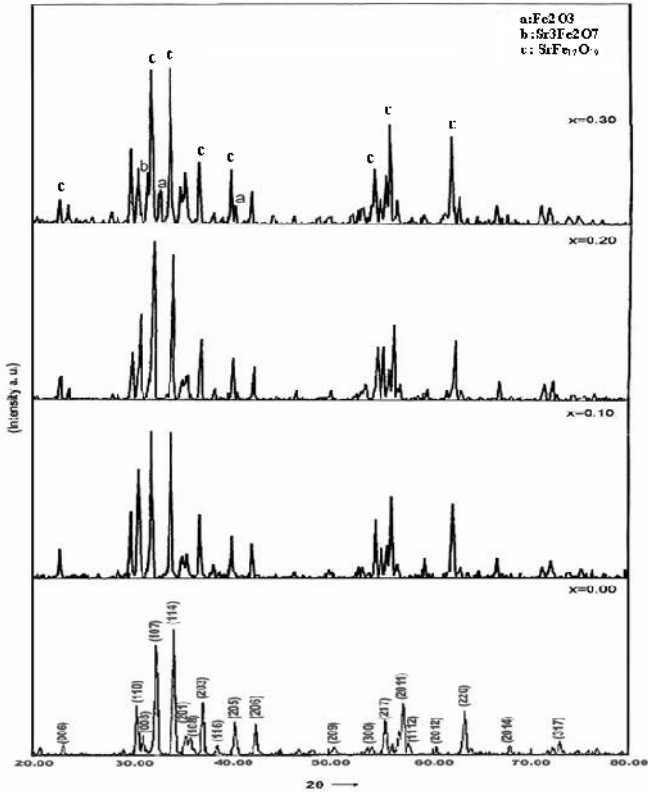


Fig. 1. XRD Patterns of  $Sr_{1-x}Dy_xFe_{12}O_{19}$  for compositions (a)  $X = 0$ , (b)  $X = 0.10$ , (c)  $X = 0.20$  and (d)  $X = 0.30$ .

**B. X-ray Density**

The X-ray density or theoretical density,  $D_x$  of all the samples was determined by the relation given in equation (1). According to which X-ray density of all the samples is directly proportional to the molecular weight of the sample and inversely proportional to the product of the lattice constant 'c' and the square of the lattice constant 'a'. As both 'a' and 'c' decrease with  $Dy^{3+}$  substitution in strontium hexaferrites, the X-ray density of these ferrites increases continuously with successive substitution of  $Dy^{3+}$  ions for  $Sr^{2+}$  ions.

**C. SEM Microstructures**

Fig. 2. Shows the microstructures of prepared samples. It indicates that the M-type ferrite grains are homogeneous hexagonal shaped crystals [15]. It was found that the average grain size estimated from SEM was approximately  $1\mu m$  and it was almost dependent on the composition  $X$  ( $x = 0.0, 0.10, 0.20$  and  $0.30$ ). The complex permeability spectra of polycrystalline ferrite depends not only on the chemical composition of the ferrite but also on the post-sintering density and the microstructures such as grain size and porosity.

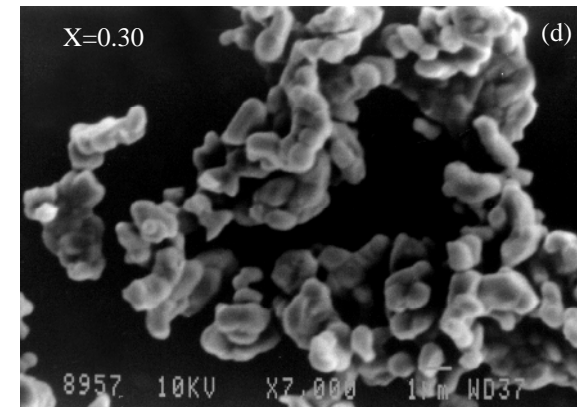
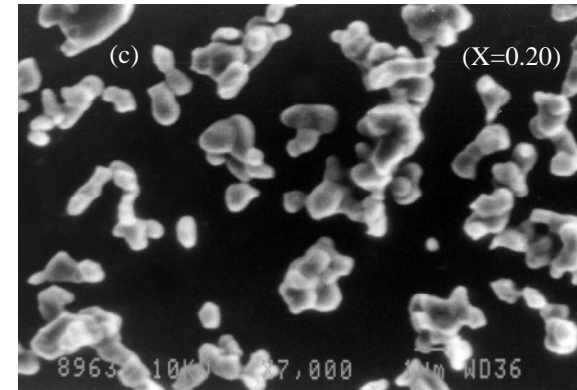
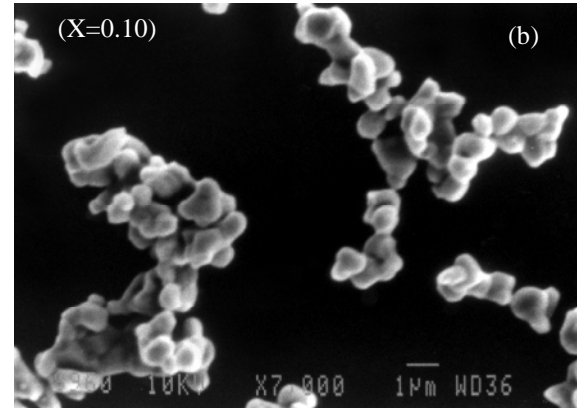
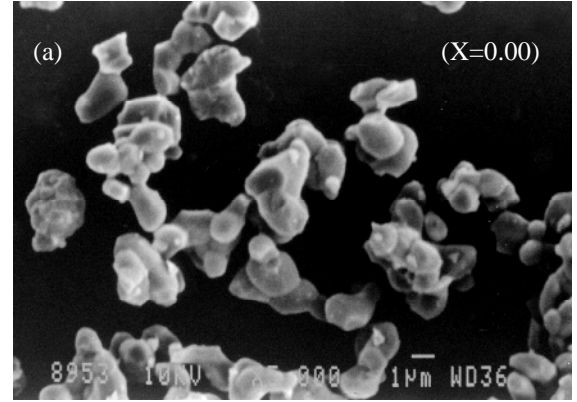


Fig. 2. SEM Photographs of  $Sr_{1-x}Dy_xFe_{12}O_{19}$  for compositions (a)  $X = 0$ , (b)  $X = 0.10$ , (c)  $X = 0.20$  and (d)  $X = 0.30$ .

#### D. Dielectric properties

The dielectric constant is the property of dielectrics, which determines the electrostatic energy per unit volume for unit potential gradient. It describes the material's capacity to store charge when it is used as a capacitor dielectric. In other words, dielectric constant is the ratio of the charge that would be stored with free space as stored with the material. The value of dielectric constant ( $\epsilon'$ ) of the ferrite samples can be calculated by using the formula

$$\epsilon' = \frac{C_p t}{\epsilon_0 A} \quad \dots (4)$$

where  $C_p$  is the capacitance of samples in pF,  $t$  is the thickness of the samples in cm,  $A$  is the cross-sectional area of the sample in  $\text{cm}^2$  and  $\epsilon_0$  is the permittivity in free space having value  $8.854 \times 10^{-12}$  pF/cm.

The variation of dielectric constant with frequency is shown in Fig. 3. It shows the dielectric constants versus frequency plots of studied sample. It is observed that all the samples show the frequency-dependent phenomenon, such that the dielectric constant decreases with increasing frequency and then reaches a constant value. The observed dispersion of the dielectric constant can be explained on the basis of the space charge polarization and hopping conduction between  $\text{Fe}^{3+}$  and  $\text{Fe}^{2+}$ . A more dielectric dispersion is observed at lower frequency range and it remains almost independent of applied external field at high frequency domain. This is due to the fact that dielectric material exhibits induced electric moment under the influence of external electric field. At higher frequency, the polarization of the induced moment could not synchronize with the frequency of applying electric field. So dielectric attains a constant value above certain high frequencies [16-17]. The polarization is governed by number of space charge carriers while take part in the ion exchange during the hopping phenomenon in  $\text{Fe}^{3+}$ - $\text{Fe}^{2+}$  or  $\text{Dy}^{3+}$ - $\text{Dy}^{2+}$  may be produced during the sintering process due to production of oxygen ion vacancies, that make the phenomenon of hopping more easier [18-23]. The dielectric dispersion is observed at low frequency-range is due to Maxwell-Wagner type interfacial polarization well in agreement with the Koops phonological theory [22-23]. According to these models, the dielectric material with a heterogeneous structure can be imagined as a structure consists of well conducting grains separated by highly resistive thin layer (grain boundaries). In this case, the applied voltage on the sample drops mainly across the grain boundaries and space charge polarization is built up at the grain boundaries. The space charge polarization is governed by the available free charges on the grain boundaries and grain boundaries are predominant at low frequencies. The thinner the grain boundary, the higher the dielectric constant. The observed decrease of  $\epsilon'$  with increasing frequency can be attributed to the fact that the electron exchange between  $\text{Fe}^{2+}$  and  $\text{Fe}^{3+}$  ions cannot follow the change of the external applied field beyond a certain frequency [19]. Basically, the whole polarization in ferrites is mainly contributed by the space charge polarization which is governed by the space charge carriers and the

conductivity of material [20-21] and hopping exchange of charge between two localized states, which is governed by the density of the localized states and resultant displacement of these charges with respect to the external field.

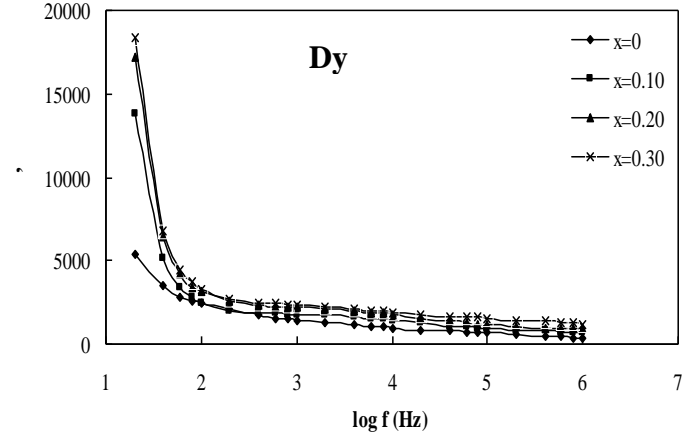


Fig. 3. Variation of dielectric constant with frequency for  $\text{Sr}_{1-x}\text{Dy}_x\text{Fe}_{12}\text{O}_{19}$  series for compositions (a)  $X = 0$  (b)  $X = 0.10$ , (c)  $X = 0.20$  and (d)  $X = 0.30$ .

Fig. 4. Shows the dispersion of dielectric loss tangent ( $\tan \delta$ ) for the studied samples at frequency range 1 KHz – 1 MHz.

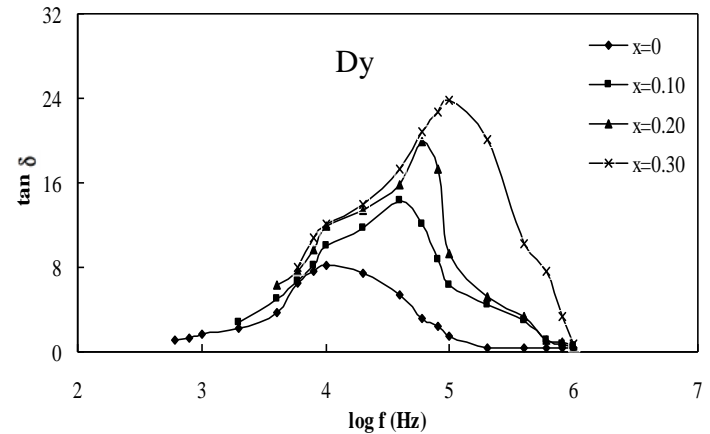


Fig. 4. Variation of dielectric loss ( $\tan \delta$ ) with frequency for  $\text{Sr}_{1-x}\text{Dy}_x\text{Fe}_{12}\text{O}_{19}$  for compositions (a)  $X = 0$ , (b)  $X = 0.10$ , (c)  $X = 0.20$  and (d)  $X = 0.30$ .

The variation of the dielectric loss tangent as a function of frequency at a constant temperature of 304 K for the series prepared with  $\text{RE} = \text{Dy}^{3+}$  are shown in Fig. 4. These figures explicitly show that the value of dielectric loss tangent increases as the frequency increases to attain its maximum (peak) value at a certain critical frequency followed by decrease at higher frequencies. The peaking behaviour in the dielectric loss occurs when the jump frequency of electron between  $\text{Fe}^{2+}$  and  $\text{Fe}^{3+}$  is equal to the frequency of the applied field [24-25].

#### IV. CONCLUSION

Addition of Dy rare earth ion strongly affect the structural and dielectric properties. This addition suppresses the abnormal grain growth and produces sub-micron grains of uniform size. Due to these structural and morphological changes, some improvement in electrical and dielectric properties has been noticed.  $Sr_{1-x}Dy_xFe_{12}O_{19}$  hexaferrite are prepared by the usual ceramic technique. From the above study, we conclude that the X-ray diffraction pattern shows that the prepared samples have a single phase structure. The lattice parameters 'c' and 'a' was found to decrease by increasing Dy-content, that enhanced the X-ray density and porosity. SEM suggested that the compound have small grains distributed on the surface of the sample and also shows the grain size has been decreases by increasing the Dy-content in the composition  $Sr_{1-x}Dy_xFe_{12}O_{19}$ . The value of dielectric constant at relatively at low frequency were very high and are attributed to the existence of interfacial polarization that arises due to in homogeneous structure of the material ensuring the presence of the secondary phases at the grain boundaries. The value of dielectric loss tangent increases as the frequency increases to attain its maximum (peak) value at a certain critical frequency followed by decrease at higher frequencies.

#### REFERENCES

- [1] G. Albnese, A. Dariu, F. Licic, S. Rinaldi, *IEEE Trans. Magn.* MAG-14 (1978) 710.
- [2]. H.J. Kown, J.Y. Shin, J.H. Oh, *J. Appl. Phys.* **75** (1994) 6109.
- [3]. E. Naiden, V. Maltsen, G. Ryabtsen, *Phys. Stat. Sol (a)* **120** (1990) 209.
- [4]. K. Yoon, D. Lee, H. Jung, S. Yoon, *J. Mater. Sci.* **27** (1992).
- [5]. S. Hussain, M.A. Rehman, A. Maqsood, M.S. Awan, *J. Cryst. Growth*, **297**(2006) 403.
- [6]. S. Hussain, A. Maqsood, *J. Magn. Magn. Mater.* **316**(2007) 73.
- [7]. S. Hussain, A. Maqsood, *Mater. Lett.*, in press.
- [8]. A.M. Ab-EI Ata, M.A. Ahmed *J. Magn. Magn. Mater* **208**(2000) 27.
- [9]. J.H. Lee, C.W. Won, *J. Kor. Inst.Met.Mater.* **33**(1995)21.
- [10]. H. Zhang, L. Li, J.Zhou, Yue, Z. Ma, Z. Gui, *J. Eur. ceram. Soc.* **21**(2001)149.
- [11]. Si-Dong Kim, Jung –Sik Kim. *Mater.* **307**(2006) 295-300.
- [12]. T. Gonzalez-Carreno, M.P. Morales, C.J. Serna, *Mater. Lett.* **43** (2000) 97.
- [13]. M.U. Rana, T. Abbas, *J. Magn. Magn. Mater.* **246**(2002)110.
- [14]. S. Hussain, A. Maqsood. *J. Magn. Magn. Mater.* **316**(2007) 73-30.
- [15]. A. Ghasemi, A. Hossienpour, A. Morisako, A. Saatchi, M. Salehi, *jmmm.* **303**(2006)429-435
- [16] K.W. Wagner, *Ann. Phys.* **40**(1913),817
- [17] V.R.K. Murthy. J. Sobhamadri, *Phys. Status Solidi* **A36**(1976)1233.
- [18] C. Parakash J.S. Baijal. *Less-Common Met* **107**(2006) 51
- [19] B.K. Kuanr, G.P.S. Tara, *Appl. Phys.* **75**(10) 2001, 6115.
- [20] A.K. Jonscher, *Dielectric Relaxation in Solids*, Chelsea Dielectrics Press, London, 1982
- [21] J. Maxwell, *Electricity and Magnetism*, Vol **1**, Oxford University Press, London, 1873
- [22] Maxwell, J.C., "Electricity and Magnetism", (Oxford) University Press, London, (1873).
- [23] Wagner, K.W., *Ann. Phys.*, **40**, 817 (1973).
- [24]. Mitra, R., Puri, R.K and Mendiratta, R.G., *J. Mater. Sci.*, **27**, 1275 (1992).
- [25]. Kolekar, C.B., Vasambekar, P.N., Kulkarni, S.G and Vaingankar, A.S., *J. Mater. Sci.*, **30**, 5784 (1995).